

Estimation of Pressure Drop of Single-Phase Flow in Horizontal Long Pipes Using Artificial Neural Network

Gharekhani, Fahime

Department of Chemical Engineering, Science and Research Branch, Islamic Azad University, Tehran, I.R. IRAN

Ardjmand, Mehdi*⁺

Department of Chemical Engineering, South Tehran Branch, Islamic Azad University, Tehran, I.R. IRAN

Vaziri, Ali

Department of Chemical Engineering, Science and Research Branch, Islamic Azad University, Tehran, I.R. IRAN

ABSTRACT: Large-pressure drops and drag along the pipe route are the problems with fluid transfer lines. For many years, various methods have been employed to reduce the drag in fluid transmission lines. One of the best ways for this purpose is to reduce friction coefficients by utilizing drag-lowering materials. Experimentally by adding minimal amounts of this material at the ppm scale to the lines and reducing the drag of the flow, fluid can be pumped without the need to change the size of the pipe. In this study, the effect of carboxymethylcellulose biopolymer on the water flow reduction in a 12.7- and 25.4-mm galvanized pipe was investigated. In order to have a comprehensive analysis of process conditions, experiments were carried out with three different levels of concentration, flow rate, and temperature. Also, as a new innovation in this investigation, the outputs of the experimental data were evaluated and analyzed using the Taguchi method and neural network system and optimized through a genetic algorithm. In this study, the highest rate of drag reduction will be achieved at 39 ° C and at a concentration of 991.6 ppm and a flow rate of 1441.1L/h was 59.83% at 12.7-mm diameter.

KEYWORDS:: Drag reduction; Pipeline; Carboxymethylcellulose; Neural network; Single phase.

INTRODUCTION

Drag reduction is an acceptable problem in the transmission of liquids through pipelines. Fluids in the upstream state generally experience drag and subsequently,

a pressure drop, which indicates a pressure drop between two points. Drag-reducing agents are generally known to have various categories such as long-chain polymers,

* To whom correspondence should be addressed.

+ E-mail: m_arjmand@azad.ac.ir

1021-9986/2022/4/1335-1347

14/\$/6.04

surfactants, particle and fiber suspensions, and compatible coating [1]. Although, Polymers having high molecular mass fluid (more than 10^6 Da) with a linear structure are considered better drag-reducing agents [2].

It is believed that drag-reducing agents work in some manner such as suppression of turbulence, laminar range limit extending to higher Reynolds Number, modification of near-wall flow, and friction reduction in completely developed turbulence flow. Polymer additives in fluid flow dampen Eddie's current formation and so the turbulence amount will be reduced[3].

There are many reviews on the effect of different variables such as concentration, diameter, length, temperature, pH, molecular weight, flexibility, and roughness, with mechanisms and models for degradable polymers [4-8]

Various aspects of this work have been investigated and tested on reducing pumping power at a constant flow rate or increasing the capacity of the pipe system at a constant pressure drop without changing pipeline conditions. In addition, studies have been carried out to better understand this phenomenon [9-14].

However, reducing drag has remained one of the challenges facing researchers, which include parameters influencing the efficiency of drag-reducing polymers, applications, and measurements of drag reductions as well as major restrictions for drag-reducing polymers in single-phase fluids[15, 16]. Wyatt et al. in 2011 [16] investigated the ability to reduce drag in the turbulent flow of channels and pipes by the addition of xanthan solution in myriad industries. They stated that drag reduction was lower through the time when diluted from an entangled stock solution but remains larger than the homogenous case after more than 24 h.

Ptasinski et al. [17, 18] reported on the observations of turbulence statistics and the various contributors to total shear stress.

Eshghinejadfard and Sharma [19] studied the effect of xanthan gum, guar flour, fiber fillers, and polyacrylonitrile fiber on pressure drop in a rectangular channel. Amarouchene et al. [20] investigated rod-like polymers to reduce drag for theoretical and experimental models. The results showed the same experimental and theoretical model performance, and the most effective polymer on drag reduction was observed by increasing Reynolds. Hong et al. [21] showed that guar gum is useful, because

it is more stable to mechanical stress than the synthetic water-soluble polymer, and they fitted the stretched-exponential model.

Yang and Dou [22] evaluated the effect of polymer on drag reduction in smooth and rough tubes, where the polymer performs better in rough tubes than in smooth tubes at the same number of Reynolds. Calzetta [23] presented theoretical studies on drag reduction by adding polymer and analyzed factors affecting drag reduction. The effect of polymer on different Reynolds was also investigated.

Salaheddin et al. [24] used coconut residue as a biopolymer in water injection systems to reduce drag. Following that, Bari et al. [25, 26] investigated the reduction of drag in the presence of aloe vera natural mucilage. He studied drag reduction with higher concentration, Reynolds number, and pipe lengths. Later, he studied the drag reduction characteristic of polyacrylamide in a rotating disk apparatus and showed that efficiency drag reduction increases with faster rotation until a maximum value then decreases. Also, degradation of high concentration matches the single exponential decay model but low concentration matches a fractional exponential model.

Perlekar et al. [27] conducted a study on the numerical simulation of statistical fluids on homogenous and isotropic liquid turbulence in the presence of polymer additives. They showed a reduction in the energy dissipation rate, a correction in the fluid energy structure specifically in the high scattering range, and a decrease in the circular flow.

Bari et al. [28] investigated the drag-reduction performance of chitosan in the turbulent flow of water. Using the various types of acid with different rate amounts of chitosan illustrates good results in decreasing drag. Moreover, drag reduction was observed to increase with DRA concentrations, although there is a critical concentration.

Abdulbari et al. [29] showed okra (*Abelmoschus esculentus*) mucilage drag reduction performance in water-soluble and oil-soluble. The drag reduction percentage was increased by higher Re by using the water solution and decreased by increasing Re when utilizing the oil soluble.

Abubakar et al. [30] studied the effect of polymer parameters such as charge density, molecular weight, and concentration. Drag reduction increases with higher

the polymer concentration in the flow reaches above 10 ppm, and increases with greater polymer molecular weight, while the maximum drag reduction was not affected by the rise in polymer charge density up to 13%. *Coelho et al.* [31] used okra fiber and mucilage to reduce drag in the high Reynolds flow tube. According to the results, the best performance is achieved at the concentration of 1600 ppm polymer. They believe that okra fiber and mucilage are better polymers because they are extraordinarily cheap and easy to be obtained. *Gasljevic et al.* [32] demonstrated that marine microalgae have a higher drag reduction efficiency than xanthan gum and polyethylene oxide, because they exhibit unusual tensile behavior of type -B, whereas xanthan gum shows behavior type-A in larger diameter and type-B in a smaller diameter. Meanwhile, microalgae of type B have high resistance to shear stress. *Karami et al.* [33] investigated the effect of using anionic copolymer SF150 (copolymer polyacrylic and acrylic acid) and polyethylene oxide and xanthan gum to reduce drag. They stated that polymer structure (softness and hardness), molecular weight, and linearity are involved in polymer decomposition rate. The order of decomposition is polyethylene oxide > copolymer > xanthan gum. In another research, he also showed a general model for predicting drag reduction in crude oil pipelines. The $f-1/2$ changes by $Ref., (1-n/2)$, where the experimental data agree well with the model. *Volokh* [34] showed that the flow stability increased with the addition of a polymer. *Zhang et al.* [35] examined the limitation of polymer drag reduction and stated that viscosity and elasticity contribute positively to drag reduction both before critical and after critical concentration. Elasticity affects the drag positively but viscosity affects it negatively. *Chai et al.* [36] conducted a study on drag reduction using an anionic polymer and surfactant mixture. Drag reduction performance obtained from the combination of anionic surfactant and anionic polyacrylamide is better than a single additive, especially under a high shear rate. According to the results, drag reduction depends on the concentration of SDS in the high range of Reynolds number, and the best drag reduction was around the polymer saturation point.

Rashid et al. [37] studied drag reduction by polyacrylamide and stated that drag reduction increased with lower crude oil viscosity. Pressure drop decreases as the concentration rises, and the pumping power and flow rate can be optimized.

Sifferman and Greenkorn [38] investigated drag reduction in three distinctly different flow systems-dilute polymer solutions, two-phase solid/liquid suspensions, and three-phase immiscible liquid/liquid flow with suspended solids. Their results show that a drag reduction of up to almost 80% was obtained for both the polymer and the oil system.

Peyghambarzadeh1 et al. [39] investigated the effect of aqueous solutions of carboxy methyl cellulose as a polymeric drag reduction agent on pressure drop and heat transfer was studied. Their results show that in laminar flow the addition of DRA increases drag reduction as well as decreases the overall heat transfer coefficient.

Vural et al. [40] in another investigation studied the effect of sodium carboxy methyl in the developed turbulent pipe flow and the impacts of increasing CMC concentration on the flow field were observed. For this purpose, they applied 200-500 mg/kg concentration and their results show that the maximum drag reduction will be archived in a high concentration (500 mg/kg).

Despite the wide range of numerical simulations and optimization methods in various fluid science fields, there are still no studies on the optimization of laboratory studies of drag reduction using genetic algorithms and neural network optimization methods as well as data analysis. Therefore, as a new study, in this paper, an experimental result has analyzed the Taguchi method and Artificial Neural Network method optimized by Genetic Algorithm (GA).

ANN coupled with GA as a powerful method can be applied for process and parameter effects modeling and optimization.

In the present study, the study of the effect of carboxymethylcellulose is recognized as a biopolymer that has no environmental contamination and does not need to be isolated from drinking water.

Carboxymethyl cellulose was measured at three concentrations of 250, 500, and 1000 ppm to reduce drag in 12.7 and 25.4 mm galvanized iron pipes at three different temperatures of 26, 36, and 46 °C, and three different flow rates of 700, 1000, and 1500 l/h. Tap water was under the below condition:

Design and analysis of the method are performed using the Taguchi method and the neural network system and genetic algorithm. Using the Taguchi method, the maximum effect was related to the concentration factor and the lowest impact to the diameter factor.

Table 1: Tap water feature.

pH	Total Hardness(ppm)	Total alkalinity
7.6	370	336

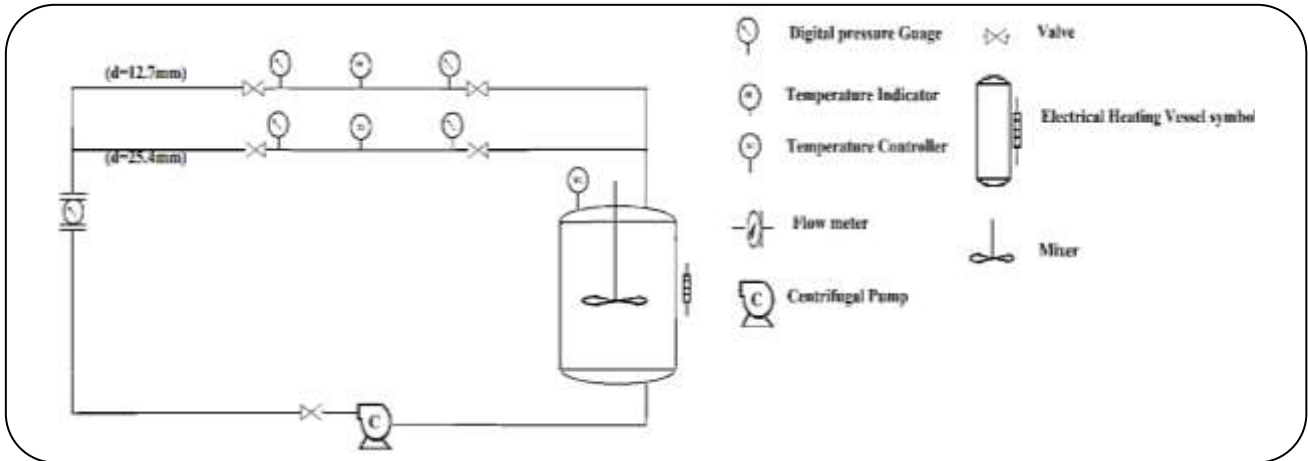


Fig. 1: Schematic diagram of the closed loop circulation system.

The definition of reducing drag phenomenon

The factors that reduce the coefficient of surface friction in the vicinity of the fluid are called perceptual factors. The method of adding additives, among them reducing factors, is of great importance. The best additives for reducing drag can be polymer additives that have sufficient degradation resistance and perform well. The injection of DRA into the pipelines destroys large vortices and becomes small vortices. As stated, the mechanism of drag reduction is still unclear and remains a significant challenge for researchers. According to *Virk et al.* [41], the thickness of the wall layer increases with the presence of DRA. This increases the layer velocity profile and consequently reduces the contact surface and friction coefficient. The results are presented in the form of an equation based on the drag reduction process. Also, it can be stated that the most significant drag reduction is observed in Reynold's currents above 2500. The percentage of drag reduction is defined as Equation (1) at a constant flow rate.

$$DR\% = \left(1 - \frac{\Delta p_{\text{polymer}}}{\Delta p_{\text{solvent}}}\right) \times 100 = \quad (1)$$

$$\left(1 - f_{\text{polymer}}/f_{\text{solvent}}\right) \times 100$$

$$f = d\Delta p / 2l\rho v^2 \quad (2)$$

d = diameter, l = length, ρ = density, v = velocity

Where $\Delta p_{\text{polymer}}$ and $\Delta p_{\text{solvent}}$ are respectively pressured drops in the polymer of additive and base fluid, and

f_{polymer} and f_{solvent} are friction coefficients in the polymer additive and the solvent.

EXPERIMENTAL SECTION

Experiment structure

In order to analyze drag reduction in a horizontal tube, the experiment has been conducted in a build-up closed-loop liquid circulatory system. The schematic diagram for the experiment is shown in Fig. 1.

It consists of two galvanized iron pipes with a diameter of 12.7 and 25.4 m. The digital pressure and temperature sensors are exactly located one meter after the first length and one meter before the last length for the purpose of eliminating input and output effects. They are connected to a tank containing a thermal element and a thermal sensor PT100, centrifugal pump (model QB60), and water flow meter.

The pressure at both sides of the tube was measured by a Trafag digital pressure sensor (application range of 0-1.6 bar and 0.01mbar accuracy-Switzerland) and read by Autonics digital display units (with an accuracy of 0.01-South Korea). Then, the pressure drop was measured, and drag reduction was calculated by Eq. (1).

The fluid inside the tank is heated by a heating element and regulated by the PT100 sensor. Also, the temperature at the two pipes has been read by the temperature sensors.

Table 2: The intended value for the input parameters.

Parameters	Level 1	Level 2	Level 3
Pipe diameter(mm)	12.7	25.4	-
Temperature(°C)	26	36	46
Concentration(ppm)	250	500	1000
Flow rate(l/h)	700	1000	1500

The flow rate was adjusted by a bass instrument flow meter (vertical rotameter) measuring from 250 to 2500 liters per hour with a precision of 5%.

Sodium carboxymethylcellulose with an average $M_w=700000$ was purchased from Sigma-Aldrich

Testing procedures

First, ensure that the inlet and outlet valves of the untested pipeline are closed and that the inlet and outlet valves of the pipeline under test are open. The single-phase flow of water without the carboxymethylcellulose enters the pipe under various operating conditions and temperatures. The parameters studied in the single-phase experiment include carboxymethylcellulose concentration, temperature, flow rate, and tube diameter. Pour the desired concentration into the tank, and heat until it reaches the desired temperature. Adjust the flow rate by opening the valves, and reading the flowmeter and the pressure on both sides using a digital pressure gauge to calculate the pressure drop and the percentage of drag reduction.

Data Analysis

In the present study, the experiment was designed using the Taguchi method and artificial neural networks, and a genetic algorithm.

Taguchi method of analysis

The Taguchi method was adopted for analysis in this experiment. The Taguchi analysis aims to obtain the best parameters of diameter, flow rate, temperature, and concentration to achieve the best DR.

The diameter of the pipe is examined at two levels, and temperature, concentration, and flow rate are at three levels. The values considered are given in Table (2). In this research, the maximum concentration of carboxymethylcellulose was adjusted to 1000 ppm. This is due to the fact that our examination range is limited to Newtonian fluids.

In similar conditions, different investigations were reported. *Abdul Bari et al.* [10, 25] obtained a maximum drag reduction of 65-65% between $Re = 7000-10000$ by using Aloe vera natural mucilage at a concentration of 400 ppm and by application of okra mucilage at a concentration of 400 ppm 60 % of drag reduction was obtained.

Hong et al. [7, 21] obtained 58% drag reduction at 1000 ppm of commercial guar gum and 65% reduction with grafted guar gum and purified guar gum. They also by using xanthan gum at 200 ppm reach 35% drag reduction.

Salaheddin et al. [24] used carboxymethylcellulose at a flow rate of m^3/h and at a concentration of 1000 ppm, reaching 38.4% drag reduction.

The related density and viscosity amount related to the experimental condition was reported in Table 3.

As can be seen from Table 4, different variables and different amounts of a selection of the four parameters according to the Taguchi algorithm are shown.

In the Taguchi method, factors or process variables are divided into two groups of controllable factors (signal) and uncontrollable factors (noise). Controllable factors are those factors that can be easily controlled and are used in the design of test processes to better choose the conditions. Uncontrollable variables or noise are all factors that are difficult to control and cause changes. The signal-to-noise ratio indicates the sensitivity of the qualitative characteristics of the factor under consideration to effective and uncontrollable external factors in a controlled process[42].

Optimal conditions are identified and determined by determining the effect of each of the input factors on the output characteristic. In general, in terms of the output characteristics of the tests, can be divided into three modes: the smaller the better, the closer to the nominal value the better, and the larger the better.

In this paper, for the analysis using the Taguchi method, the the-larger-the-better mode is chosen. This means

Table 3: Characteristics of fluid in different condition.

Polymer concentration	T=26 °C		T=36 °C		T=46 °C	
	Density(g/mL)	Viscosity (mpa.s ×10 ⁻³)	Density(g/mL)	Viscosity (mpa.s ×10 ⁻³)	Density(g/mL)	Viscosity (mpa.s ×10 ⁻³)
250	0.997811	0.907	0.994654	0.712	0.989854	0.563
500	0.997922	1.023	0.99477	0.773	0.989907	0.636
1000ppm	0.998057	1.184	0.994834	0.92	0.990885	0.745

Table 4: Different amounts considered by the Taguchi method and %DR.

Diameter(C1)	Temperature (C2)	Concentration(C3)	Flow rate(C4)	Related Reynolds	Drag reduction percentage	P water (mbar) Δ	P polymer(mbar)Δ
12.7	26	250	700	21515.96	8.7	30	27.39
12.7	36	500	1000	35857.79	32.0	64	43.52
12.7	46	1000	1500	54743.11	60.0	153	61.2
12.7	26	250	700	21515.96	8.7	30	27.39
12.7	36	500	1000	35857.79	32.0	64	43.52
12.7	46	1000	1500	54743.11	60.0	153	61.2
12.7	26	250	1000	30653.25	11.0	94	83.66
12.7	36	500	1500	53606.9	34.0	153	100.98
12.7	46	1000	700	26013.45	42.8	34	19.45
12.7	26	250	1500	45826.19	17.0	157	130.31
12.7	36	500	700	25169.1	27.0	31	22.63
12.7	46	1000	1000	37060.16	53.6	71	32.94
12.7	26	500	1500	40633.94	29.0	157	111.47
12.7	36	1000	700	21148.87	38.0	31	19.22
12.7	46	250	1000	48989.51	12.0	71	62.48
12.7	26	500	1500	40633.94	29.0	157	111.47
12.7	36	1000	700	21148.79	38.0	31	19.22
12.7	46	250	1000	48989.5	12.0	71	62.48
25.4	26	500	700	9514.4	10.9	5	4.46
25.4	36	1000	1000	15051.4	39.3	7	4.25
25.4	46	250	1500	36753.3	31.5	14	9.59
25.4	26	500	1000	54360.29	11.3	11	9.76
25.4	36	1000	1500	22603.8	41.2	16	9.41
25.4	46	250	700	17148.56	20.0	3	2.4
25.4	26	1000	1000	11733.74	38.5	11	6.76
25.4	36	250	1500	29359.83	23.2	16	12.29
25.4	46	500	700	15181.06	18.5	3	2.44
25.4	26	1000	1000	11733.24	38.5	11	6.77
25.4	36	250	1500	29202.87	22.0	16	12.48
25.4	46	500	700	15181.06	18.5	3	2.44
25.4	26	1000	1500	17621.3	40.0	6	3.6
25.4	36	250	700	13625.67	10.7	3	2.68
25.4	46	500	1000	21664.64	22.0	10	7.8
25.4	26	1000	700	8221.83	35.0	5	3.25
25.4	36	250	1000	19444.93	16.2	7	5.87
25.4	46	500	1500	32536.5	30.0	14	9.8

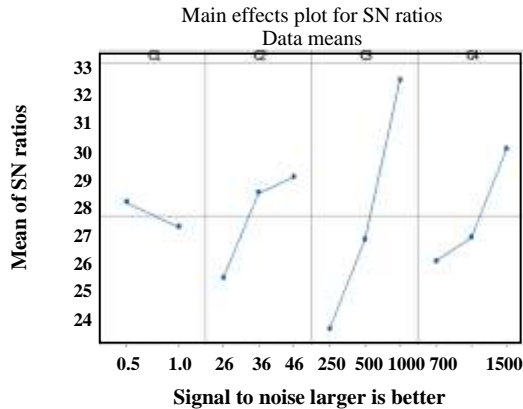


Fig. 2: mean of the S/N ratios for each factor based on the signal-to-noise larger is better.

that greater drag reduction results in a better output from selecting the desired parameters.

As evident in the results of Fig. 2, the diameter of the pipe has the least effect on drag reduction while concentration has the highest efficiency. However, temperature and flow rate have a similar impact, and concentration, flow rate, the temperature at level 3, and diameter at level 1 have the maximum percentage of drag reduction.

Analysis of results using artificial neural networks and genetic algorithm

In most engineering design issues, the relationship between the objective function, and the design variables is not analytically available, and many experiments or simulations are needed to identify and determine this relationship.

In most cases, each of these tests and simulations is expensive and time-consuming. As a result, optimization, searching for meaning design, and sensitivity analysis, where the target function is read thousands and even millions of times, seems impossible. However, in recent years, neural networks have emerged as one of the most important surrogate models of outstanding performance, particularly in applications such as pattern recognition and function approximation. These networks are capable of learning the complex nonlinear relationships between input and output variables of a system without prior knowledge of that phenomenon or system. Artificial neural networks are ideas inspired by the biological nervous system for information processing. The neuron is the smallest unit of an artificial neural network [43, 44].

The structure of an artificial neuron is shown in Fig. 3. A layer arises from a community of multiple neurons that operate in parallel. Each layer has its function, and the artificial neural network is created by combining the layers. In general, there are three types of neuronal layers in artificial neural networks: 1. an input layer; 2. one or more hidden layers; and 3. an output layer. Both layers of a network are connected by weights and indeed, connections. The weights are first randomly assigned and then determined during the learning process by reducing the correction line and their final values. There are no specific rules for selecting and quantifying the number of neurons in the neural network layer [45, 46]. There are various types of artificial neural networks based on how neurons interact, such as the perceptron networks, Hutchinson, etc.

Usually, the R^2 coefficient is used to determine the performance of the model. In the neural network, R^2 determines the accuracy of the model in predicting outputs.

$$R^2 = 1 - \frac{\sum (Y_R - Y_S)^2}{\sum \left(Y_R - \frac{\sum Y_R}{N} \right)^2}$$

Y_S , Y_R , N are the actual data, the simulated (predicted) data, and the total number of data used, respectively. In many models, the R^2 coefficient cannot express the performance of the model alone. Therefore, other parameters such as RMSE (Root mean square error) and ARD (average relative deviation) are proposed:

where,

$$ARD\% = \sum_{i=1}^n \left(\frac{|(y_R - y_s)|}{n \cdot y_s} \right) \times 100$$

$$RMSE = \left(\sum_{i=1}^n (y_R - y_s) / n \right)^{1/2}$$

The mean square root of the mean squared error is the difference between the value of experiments and the prediction model amount. In this article, the combination of ANN and genetic algorithms is used. Temperature, concentration, flow rate, and diameter were also used to find the optimum values. First, the optimal structure for the above four values is obtained using the ANN model and the optimal amount of drag reduction is obtained using the GA model and fitness function.

Optimization was performed by a genetic algorithm using the GA in Toolbox of Matlab.

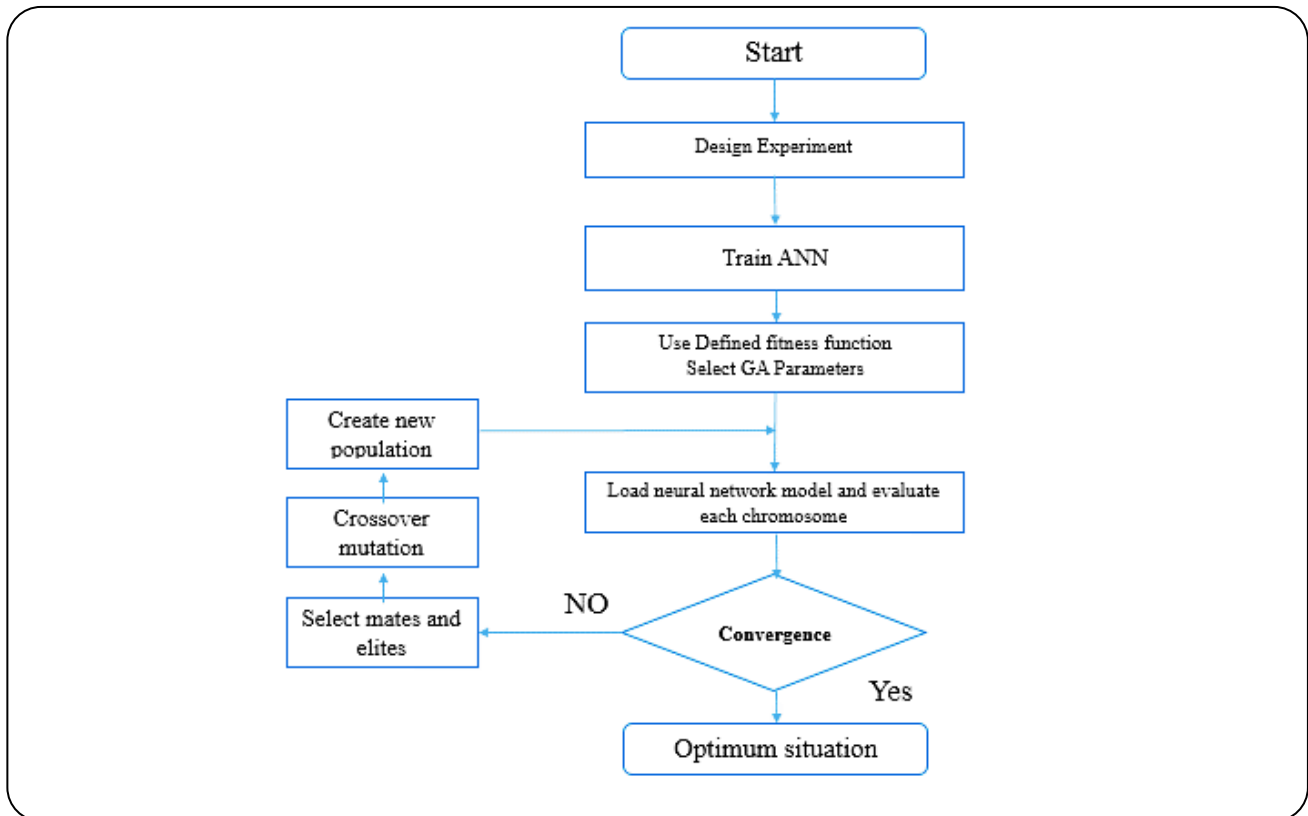


Fig. 3: Considered Model for combining genetic algorithm with a neural network.

The flowchart using the ANN-GA hybrid model is given above.

RESULTS AND DISCUSSIONS

ANN modeling

In this section, pipe diameter, temperature, concentration, and flow rate are considered as input parameters using the multilayer forward model. Initially, training data, including input and target values, were correlated with laboratory results. A set of input and output data is required for the ANN (Artificial neural network) model. Training data is used in network training, weight calculation, and composing the network parameters.

We assume that a Multi-Layer Perceptron (MLP) with a hidden layer works as well as a corresponding MLP with more than one hidden layer in problem-solving. However, there is no general rule for obtaining the number of hidden layers. Based on this fact, a single hidden layer was selected for model development [47-52]. As mentioned before, few neurons weaken the input and output modeling relationships, while using too many neurons may also cause over-fitting. For this purpose, the number of neurons in this layer is considered a parameter for developing

the ANN model. The ANN model, which is discussed in this study, involves a large number of neurons. The link strengths vary between neurons, and the neurons' passing signals had different weights, consequently. In this paper, the validation was performed by the method of k-fold, and the choice of 8 cross-validations. Validation data has been used to ensure the improvement of the modeling with ANN and the prevention of overfitting. Test data were used to evaluate and validate the model produced. The number of optimized neurons in the ANN model is given below. For this purpose, the number of hidden layers ranges from 5 to 10 variables. According to Fig. 4, the best network performance is obtained at the number of 8 neurons in the hidden layer.

The following is a graphical view of the designed grid (Fig. 5).

The relative importance of each variable is shown in Fig. 6. The figure shows the output impact of each variable. In general, the drag effect is higher than the concentration of all parameters, and the pipe diameter has the least efficiency on the drag. The flow rate and temperature are in the following order after concentration.

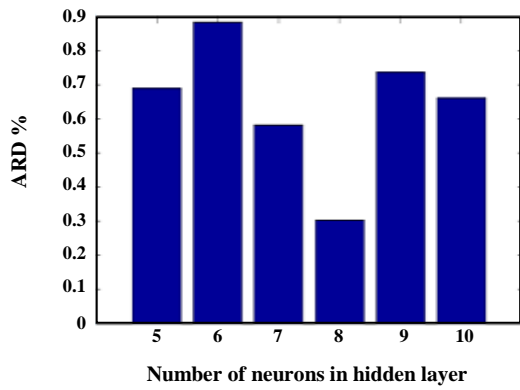


Fig. 4: ARD versus the number of neurons in the hidden layer.

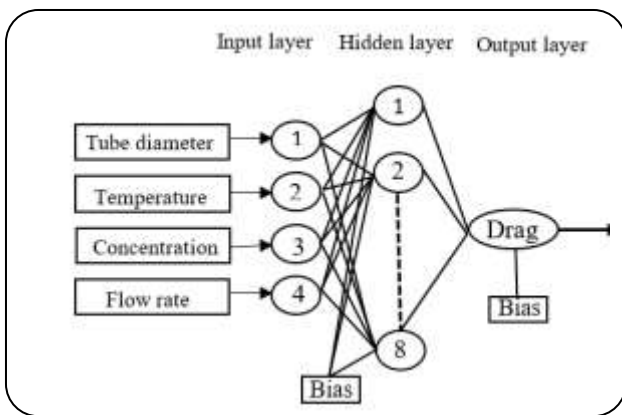


Fig. 5: Neural network topology, inputs, and outputs connected through a hidden layer.

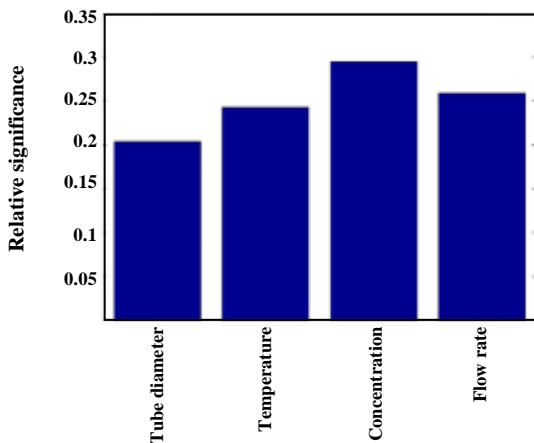


Fig. 6: Relative significance of input parameters on Drag.

The network parameters are measured to evaluate the neural network after finding the best topology. The values of the parameters are given in the following table for the three layers.

Table 4: Test data in each category for the 8-fold cross validation method.

Category	Test data						
	1	60	12	29	20	23.2	38.5
2	60	29	41.2	38.5	23.2	18.5	40
3	32	8.7	60	29	38.5	22	40
4	11	29	38	10.9	38.5	22	22
5	8.7	60	32	34	12	22	22
6	8.7	12	29	38	31.5	38.5	23.2
7	32	8.7	38	31.5	41.2	22	30
8	60	12	29	20	23.2	38.5	22

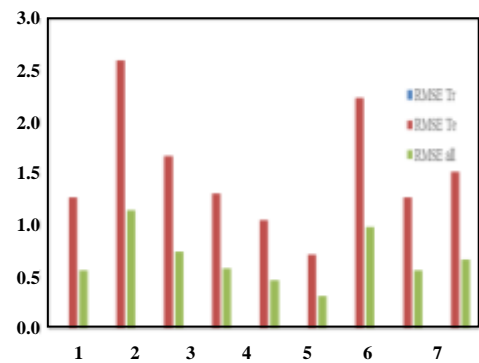


Fig. 7: RMSE values of each selected fold in an 8-fold cross-validation method for optimal topology.

The test data in each section is shown in Table 4.

Fig. 7 shows the corresponding RMSE values for training and testing all data in different subsets along with the average values. Insignificant variation in the amount of RMSE causes strong generalization ability for different sections representing the selected structure (4.8.1). It should be mentioned that the RMSE train value is close to zero.

Fig. 8 shows the predicted percentage of drag reduction versus the empirical values, which have been gathered for training and testing all data. The resulting value for R^2 shows that the created network was properly trained.

The data R^2 shows that the predicted drag reduction complies with the measured one.

The error histogram can be used for showing the error dispersal from predicted values ($error = (y_{nn} - y_{exp})$).

The near-zero disturbance value shows a high reliability of the generated model (Fig. 9).

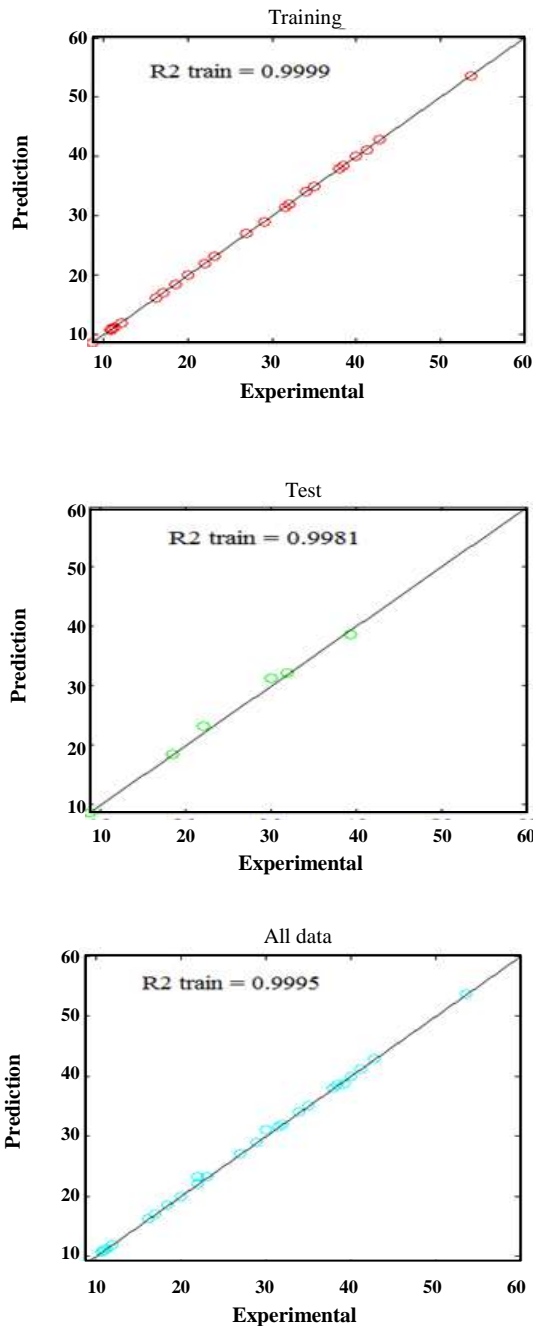


Fig. 8: Experimental values versus prediction.

Table 5 also presents the optimal parameters obtained for RMSE, R^2 , and ARD.

Modeling and optimization

As stated above, the main purpose of this study is to determine the optimal parameters to obtain the most drag

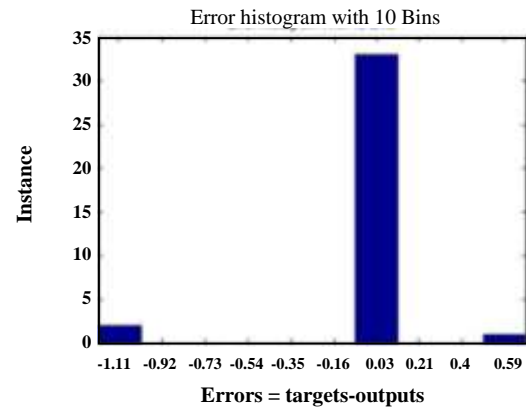


Fig. 9: Error disturbance histogram.

reduction using a genetic algorithm. Therefore, the optimization results are obtained from the genetic algorithm method using the coding model in Matlab. The starting and ending values for the effective parameters are given in Table 6.

The optimum values for pipe diameter, temperature, concentration, and flow rate were obtained after applying the above conditions and executing the optimization program, as shown in Table 7.

The chart of fitness values is shown below (Fig. 10). Optimization results have been achieved in 51 generations.

Parameters affect interpretation

The results are in accordance with theoretical facts that as the pipe diameter decreases, the drag reduction increases. This phenomenon is due to the fact that by pipe diameter reduction, the relative roughness increases which results in higher turbulence and more drag reduction. Also, it is shown that by increasing temperature to the optimum amount the drag reduction increases. This observation may be related to the fact that temperature increases until optimum temperature the DRA solubility enhance but by more increase polymer degradation is possible. Also as it is observed by DRA concentration in the investigated range increase the drag reduction increase. It is due to the fact that by increasing the concentration of additives more chains of polymers will be increased and so dampening the formation of Eddie's current and drag reduction increases. Also as shown by the flow rate increases the drag reduction also increases. Since the flow turbulence degree increase by increasing the fluid velocity it is expected that drag reduction enhance in the same manner[3, 53].

Table 5: Performance of optimum ANN model (carboxymethylcellulose).

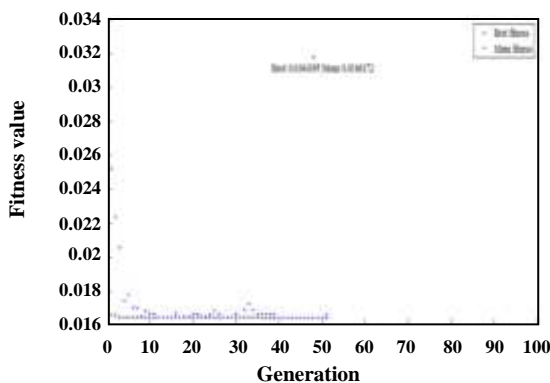
Source	Training	Test	All
R ²	0.9999	0.9981	0.9995
RMSE	6.0304×10 ⁻¹⁴	0.6721	0.2964
ARD	1.8240×10 ⁻¹³	1.5612	0.6901

Table 6: Lower bound and upper bound should have been mentioned.

Parameters	Lower bound	Upper bound
Tube Diameter	12.7	25.4
Temperature	26	46
Concentration(ppm)	250	1000
Flow rate (l/h)	700	1500

Table 7: Optimum condition obtained GA for carboxyl: 59.97%

Parameters	Optimum value
Tube Diameter [37]	12.7
Temperature (o C)	39.143
Concentration(ppm)	991.611
Flow rate(l/h)	1441.08

**Fig. 10: The best condition has been achieved in 51 generations.**

CONCLUSIONS

In the present study, a single-phase fluid flow laboratory model was designed. Carboxyl methylcellulose was used as a drag-reducing material, which is a natural biopolymer and biodegradable, as an important component of this study. The pipes were made of galvanized steel

in two diameters of 12.7 and 25.4 mm. Experiments were carried out for three different temperatures, concentrations, and flow rates. The results of the Taguchi method were analyzed, which show the strong effect of concentration on drag reduction compared to other influencing parameters. The results were optimized using a hybrid neural network model and genetic algorithm to better analyze the parameters. The obtained RSME and R² parameters indicate the optimal training of the generated neural network. Also, optimum values of 12.7, 1441.08, 991.611, 39.143 were obtained for pipe diameter, flow rate, concentration, and temperature, respectively. Finally, a 59.97% drag reduction was achieved by applying optimal conditions for unchanged input parameters to other equipment such as pumps.

Received : Oct. 28, 2020 ; Accepted : May 31, 2021

REFERENCES

- [1] Mowla D., Naderi A., [Experimental study of Drag Reduction by a Polymeric Additive in Slug Two-Phase Flow of Crude Oil and Air in Horizontal Pipes](#), *Chem. Eng. Sci.*, **61(5)**:1549-1554 (2006).
- [2] Karami H., Mowla D., [Investigation of the Effects of Various Parameters on Pressure Drop Reduction in Crude Oil Pipelines by Drag Reducing Agents](#), *J. Non-Newtonian Fluid Mech.*, **177**: 37-45 (2012).
- [3] Mucharam L., Rahmawati S., Ramadhani R., [Drag Reducer Selection for Oil Pipeline Based Laboratory Experiment](#), *Mod. Appl. Sci.*, **12(1)**: 112 (2017).
- [4] Karami H., Mowla D., [A General Model for Predicting Drag Reduction in Crude Oil Pipelines](#), *J. Pet. Sci. Eng.*, **111**: 78-86 (2013).
- [5] Wang Y., Yu B., Zakin J L., Shi H., [Review on Drag Reduction and its Heat Transfer by Additives](#), *Adv. Mech. Eng.*, **3**:478749 (2011).
- [6] Han W.J., Dong Y.Z., Choi H.J., [Applications of Water-Soluble Polymers in Turbulent Drag Reduction](#), *Processes*, **5(2)**: 24 (2017).
- [7] Hong C.H., Jang C.H., Choi H.J., [Turbulent Drag Reduction with Polymers in Rotating Disk Flow](#), *Polymers*, **7(7)**: 1279-1298 (2015).
- [8] Abubakar A., Al-Wahaibi T., Al-Wahaibi Y., Al-Hashmi A., Al-Ajmi A., [Roles of Drag Reducing Polymers in Single-and Multi-Phase Flows](#), *Chem. Eng. Res. Des.*, **92(11)**:2153-2181 (2014).

- [9] Gierczycki A., Drzazga M., Lemanowicz M., Dzido G., [Drag Reduction in the Flow of CuO Based Nanofluid](#), *Inżynieria i Aparatura Chemiczna*, **(1)**: 8-9 (2015).
- [10] Bari H A., Ahmad M., Yunus R., [Formulation of Okra-Natural Mucilage as Drag Reducing Agent in Different Size of Galvanized Iron Pipes in Turbulent Water Flowing System](#), *J. App. Sci(Faisalabad)*, **10(23)**: 3105-3110 (2010).
- [11] Al-Yaari M., Soleimani A., Abu-Sharkh B., Al-Mubaiyedh U., Al-Sarkhi A., [Effect of Drag Reducing Polymers on Oil-Water Flow in a Horizontal Pipe](#), *Int. J. Multiphase Flow*, **35(6)**:516-524 (2009).
- [12] Edomwonyi-Otu L., Chinaud M., Angeli P., [Effect of Drag Reducing Polymer on Horizontal Liquid-Liquid Flows](#), *Exp. Therm. Fluid Sci.*, **64**: 164-174 (2015).
- [13] Jafari A., Shahmohammadi A., Mousavi S M., [CFD Investigation of Gravitational Sedimentation Effect on Heat Transfer of a Nano-Ferofluid](#), *Iran. J. Chem. Chem. Eng. (IJCCE)*, **34(1)**: 87-96 (2015).
- [14] Mohebbi K., Rafee R., Talebi F., [Effects of Rib Shapes on Heat Transfer Characteristics of Turbulent Flow of Al₂O₃-Water Nanofluid Inside Ribbed Tubes](#), *Iran. J. Chem. Chem. Eng. (IJCCE)*, **34(3)**: 61-77 (2015).
- [15] Rashed M.K., Mohd Salleh M.A., Abdulbari H.A., Ismail M.H.S., [Enhancing the Drag Reduction Phenomenon within a Rotating Disk Apparatus Using Polymer-Surfactant Additives](#), *Appl. Sci.*, **6(12)**: 355 (2016).
- [16] Wyatt N.B., Gunther C.M., Liberatore M.W., [Drag Reduction Effectiveness of Dilute and Entangled Xanthan in Turbulent Pipe Flow](#), *J. Non-Newtonian Fluid Mech.*, **166(1-2)**: 25-31 (2011).
- [17] Patasinski P., Boersma B., Nieuwstadt F., Hulsen M., Van den Brule B., Hunt J., [Turbulent Channel Flow Near Maximum Drag Reduction: Simulations, Experiments and Mechanisms](#), *J. Fluid Mech.*, **490**: 251-291 (2003).
- [18] Patasinski P., Nieuwstadt F., Van Den Brule B., Hulsen M., [Experiments in Turbulent Pipe Flow with Polymer Additives at Maximum Drag Reduction](#), *Flow, Turbul. Combust.*, **66(2)**: 159-182 (2001).
- [19] Eshghinejadfard A., Sharma K., Thévenin D., [Effect of Polymer and Fiber Additives on Pressure Drop" in a Rectangular Channel](#), *J. Hydrodyn*, **29(5)**:871-878 (2017).
- [20] Amarouchene Y., Bonn D., Kellay H., Lo T-S., L'vov V.S., Procaccia I., [Reynolds Number Dependence of Drag Reduction by Rodlike Polymers](#), *Phys. Fluids*, **20(6)**: 065108 (2008).
- [21] Hong C., Zhang K., Choi H., Yoon S., [Mechanical Degradation of Polysaccharide Guar Gum Under Turbulent Flow](#), *J. Ind. Eng. Chem.*, **16(2)**: 178-180 (2010).
- [22] Yang S., Dou G., [Turbulent Drag Reduction with Polymer Additive in Rough Pipes](#) (2010).
- [23] Calzetta E., [Drag Reduction by Polymer Additives From Turbulent Spectra](#), *Phys. Rev. E.*, **82(6)**: 066310 (2010).
- [24] Salehudin S.S., Ridha S., [Coconut Residue as Biopolymer Drag Reducer Agent in Water Injection System](#), *Int. J. Appl. Eng. Res.*, **11(13)**: 8037-8040 (2016).
- [25] Bari H.A., Letchmanan K., Yunus R.M., [Drag Reduction Characteristics Using Aloe Vera Natural Mucilage: An Experimental Study](#), *J. Appl. Sci.*, **11(6)**:1039-1043 (2011).
- [26] Bari H.A.A., Yousif Z., Acoob Z.B., [Drag Reduction Characteristics of Polyacrylamide in a Rotating Disk Apparatus](#), *Res. J. Appl. Sci., Eng. Technol.* **12(10)**: 1025-1030 (2016).
- [27] Perlekar P., Mitra D., Pandit R., [Direct Numerical Simulations of Statistically Steady, Homogeneous, Isotropic Fluid Turbulence with Polymer Additives](#), *Phys. Rev. E*, **82(6)**: 066313 (2010).
- [28] Bari H A., Mohamad N., Mohd N., Nour A., [Effect of Chitosan Solution in Turbulent Drag Reduction in Aqueous Media Flow](#), *Sci. Res. Essays*, **6(14)**: 3058-3064 (2011).
- [29] Abdulbari H.A., Kamarulizam N.S., Nour A., [Grafted Natural Polymer as New Drag Reducing Agent: An Experimental Approach](#), *Adv. Mech. Eng.*, **18(3)**: 361-371 (2012).
- [30] Abubakar A., Al-Hashmi A., Al-Wahaibi T., Al-Wahaibi Y., Al-Ajmi A., Eshrati M., [Parameters of Drag Reducing Polymers and Drag Reduction Performance in Single-Phase Water Flow](#), *Adv. Mech. Eng.*, **6**: 202073 (2014).
- [31] Coelho E.C., Barbosa K.C., Soares E.J., Siqueira R.N., Freitas J.C., [Okra as a Drag Reducer for High Reynolds Numbers Water Flows](#), *Rheol. Acta*, **55(11-12)**:983-991 (2016).

- [32] Gasljevic K., Hall K., Chapman D., Matthys E., Invariant Type-B Characteristics of Drag-Reducing Microalgal Biopolymer Solutions, *Exp. Fluids*, **58**(5): 54 (2017).
- [33] Karami H R., Rahimi M., Ovaysi S., Degradation of Drag Reducing Polymers in Aqueous Solutions, *Korean J. Chem. Eng.*, **35**(1):34-43 (2018).
- [34] Volokh K., An Explanation of the Drag Reduction Via Polymer Solute, *Acta Mech.*, **229**(10): 4295-4301 (2018).
- [35] Zhang X., Duan X., Muzychka Y., Analytical Upper Limit of Drag Reduction with Polymer Additives in Turbulent Pipe Flow, *J. Fluids Eng.*, **140**(5): - (2018).
- [36] Chai Y., Li X., Geng J., Pan J., Huang Y., Jing D., Mechanistic Study of Drag Reduction in Turbulent Pipeline Flow over Anionic Polymer and Surfactant Mixtures, *Colloid Polym. Sci.*, **297**(7-8): 1025-1035 (2019).
- [37] Rashid F., Azziz H N., Talib S M., Experimental Investigation of Drag Reduction by a Polymeric Additive in Crude Oil Flow in Horizontal Pipe, *J. Ad. Res. Fluid. Mech. Therm. Sci.*, **60**(1): 15-23 (2019).
- [38] Sifferman TR., Greenkorn RA., Drag Reduction in Three Distinctly Different Fluid Systems, *Soc. Pet. Eng. J.*, **21**(06): 663-669 (1981).
- [39] Peyghambarzadeh S.M., Hashemabadi S.H., Saffarian H., Shekari F., Experimental Study of the Effect of Drag Reducing Agent on Pressure Drop and Thermal Efficiency of an Air Cooler, *J. Heat Mass Transfer.*, **52**(1): 63-72 (2016).
- [40] Vural Ş.Z., Bayram G., Uludağ Y., Experimental Investigation of Drag Reduction Effects of Polymer Additives on Turbulent Pipe Flow Using Ultrasound Doppler Velocimetry, *Turk. J. Chem.*, **38**(1): 142-151 (2014).
- [41] Virk P S., Drag Reduction Fundamentals, *AIChE J.*, **21**(4): 625-656 (1975).
- [42] Panahi P.N., Salari D., Niaei A., Mousavi S.M., Study of M-ZSM-5 Nanocatalysts (M: Cu, Mn, Fe, Co...) for Selective Catalytic Reduction of NO with NH₃: Process Optimization by Taguchi Method, *Chin. J. Chem. Eng.*, **23**(10):1647-1654 (2015).
- [43] Hajela P., Berke L., Neural Networks in Structural Analysis and Design: An Overview, *Comp. Syst. Eng.*, **3**(1-4): 525-538 (1992).
- [44] Haykin S., Network N., A Comprehensive Foundation, *Neural Networks*, **2**: 41 (2004).
- [45] Ehsani M.R., Bateni H., Parchikolaei G.R., Modeling the Oxidative Coupling of Methane Using Artificial Neural Network and Optimizing of its Operational Conditions Using Genetic Algorithm, *Korean J. Chem. Eng.*, **29**(7): 855-861 (2012).
- [46] Song K-S., Kang S-O., Jun S-O., Park H-I., Kee J-D., Kim K-H., Lee D-H., Aerodynamic Design Optimization of Rear Body Shapes of a Sedan for Drag Reduction, *Int. J. Auto. Tech.*, **13**(6): 905-914 (2012).
- [47] Basheer I A., Hajmeer M., Artificial Neural Networks: Fundamentals, Computing, Design, and Application, *J. Microbiol. Methods*, **43**(1): 3-31 (2000).
- [48] Bixler G D., Bhushan B., Fluid Drag Reduction and Efficient Self-Cleaning with Rice Leaf and Butterfly Wing Bioinspired Surfaces, *Nanoscale*, **5**(17):7685-7710 (2013).
- [49] Davis L., Handbook of Genetic Algorithms (1991).
- [50] Soleimanzadeh H., Niaei A., Salari D., Tarjomannejad A., Penner S., Grünbacher M., Hosseini S A., Mousavi S M., Modeling and Optimization of V2O5/TiO2 Nanocatalysts for NH₃-Selective Catalytic Reduction (SCR) of NO_x by RSM and ANN Techniques, *J. Environ. Manage.*, **238**: 360-367 (2019).
- [51] Mehralizadeh A., Derakhshanfard F., Ghazi Tabatabaei Z., Applications of Multi-Layer Perceptron Artificial Neural Networks for Polymerization of Expandable Polystyrene by Multi-Stage Dosing Initiator, *Iran. J. Chem. Chem. Eng., (IJCCE)*, **41**(3): 890 - 901 (2022).
- [52] Zarei M., Pezhhanfar S., Shekaari Teymourloue T., Khalilzadeh M., Neural Network, Isotherm and Kinetic Study for Wastewater Treatment Using Populus Alba's Pruned Material, *Iran. J. Chem. Chem. Eng., (IJCCE)*, **40**(6): 1868-1881 (2020)
- [53] Pouranfard A., Mowla D., Esmailzadeh F., An Experimental Study of Drag Reduction by Nanofluids Through Horizontal Pipe Turbulent Flow of a Newtonian Liquid, *J. Ind. Eng. Chem.*, **20**(2): 633-637 (2014).